J Solid State Electrochem (1998) 2: 50–57

ORIGINAL PAPER

Vladimir E. Vigdergauz · Tatyana V. Nedosekina

The wettability of electrodes made of natural metal sulfides

Received: 28 February 1997 / Accepted: 12 August 1997

Abstract Experimental methods for the evaluation of the wettability of electrodes made from natural mineral sulfides are discussed for the case of potentiostatic polarization. The wettability, induced by xanthates with different lengths of the alkyl chain, was studied for the case of pyrite, chalcopyrite, galena, arsenopyrite and chalcocite. Therefore measurements of the detachment force of an air bubble (ABDF) and of the induction time (ABIT) were performed. The first of these allows us to estimate the conditions for the destruction of the bubble-mineral complex, and the second allows us to estimate the conditions of aggregate formation under collision. The study was carried out at various polarization potentials in a borate buffer solution. The results of the measurements are compared with thermodynamic data and with experimental results obtained for representative cases such as xanthate sorption and flotation recovery. A correlation of the flotation experiments with the ABDF results can be demonstrated.

Key words Sulfide minerals · Wettability · Electrochemistry · Bubble detachment · Induction time

Introduction

Sulfide minerals form the main source of copper, lead, zinc and other non-ferrous metals. They possess relatively high conductivity and photo- and catalytic activities. The main industrial processes of sulfide treatment – froth flotation and hydrometallurgical stages – include electrochemical reactions such as catalytic electroreduction of dissolved oxygen and sulfide oxidation [1–3]. The electrochemical nature of the elementary processes of ore treatment is nowadays generally recognised. The rates of the elementary processes of hydrometallurgical treatment are very much influenced by the wettability of the mineral phases. Froth flotation results are determined by the interaction of air bubbles with the mineral particles. The achievement of different hydrophobicities of different minerals is a key to gaining higher selectivities in flotation. In this paper, an attempt has been made to discuss the influence of the electrochemical potential and amount of flotation collector consumption on the wettability of electrodes of natural sulfide minerals.

The wettability of a surface is usually estimated by measuring contact angles. The relationship between the wetting contact angle and the surface tensions or surface free energies at interfaces are described by the capillary equation of Young [4]:

$$\sigma_{sl} - \sigma_{sv} + \sigma_{lv} \cos\theta = 0, \quad (1)$$

where $\sigma_{sl}, \sigma_{sv}, \sigma_{lv}$ are the surface tensions for solid-liquid, solid-vapour and liquid-vapour interfaces, respectively, and θ is the contact angle.

According to Young's equation, for a wetting decrease it is necessary to increase the surface tension of the solid-liquid and liquid-vapour interfaces.

A direct measurement of the influence of the potential of metallic electrodes on their wettability shows that the electrocapillary curve describes the changes of σ_{sl} [5]. The σ_{sl} decreases in both directions from the potential of zero charge. Electrochemical polarization does not influence the surface free energy of a liquid-gas interface. In the first approximation it does not change the magnitude of σ_{sv}. The surface energy of the solid-liquid interface, and hence also the contact angle, will decrease upon increasing cathodic or anodic polarization. That leads to a decrease of the detachment force. As a result, the contact angle and the detachment force reach their maximum at zero surface charge.

V.E. Vigdergauz (✉) · T.V. Nedosekina
Institute of Complex Exploitation of Mineral Resources,
Russian Academy of Sciences, IPKON RAN,
4 Kryukovsky, 111020 Moscow, Russia
Tel.: +7-095-360-89-64; Fax: 7-095-360-89-60;
e-mail: vigderg@rinet.ru

In comparison with an ideally polarizable mercury electrode, the situation is more complex in the case of sulfide minerals. A polarization can easily lead to irreversible qualitative and quantitative changes of the composition of their surface [6–8]. In the presence of water and oxygen, sulfides are thermodynamically unstable. They tend to form oxides, hydroxides, and a variety of sulfur compounds. Sulfide oxidation is known to be a rather slow process. This is the reason for the existence of sulfides in ore bodies and in flotation tails stored for many years. The oxidation of sulfides provides both hydrophilic (oxides and hydroxides) and hydrophobic (elemental sulfur and sulfur excess metal sulfides) products. Therefore, their oxidation can lead (depending on conditions) to hydrophilic or hydrophobic surfaces. The addition of different surface-active organic substances to a solution leads to changes of surface free energy at all three interfaces. This can remarkably change the wettability of the surfaces. Redox transitions of the reagents (e.g. the oxidation of xanthate to dixanthogen) can lead to additional complications [9, 10]. As a result of a continuous oxidation of the sulfides and sorption of reagents (modifiers and collectors) on their surfaces, the surface composition will change. The same processes and a possible dissolution and hydrolysis of reagents will lead to a change of the composition of the liquid phase too. Further, as a result of a cathodic reduction of oxygen, accompanied by an oxidation of the sulfide minerals and the thiol collectors, the composition of the gas phase may also change. These reactions proceed continuously and at different rates.

The contact angle of the bubble/mineral/solution interface has been employed for many years as a measure of hydrophobicity of mineral surfaces and, hence, of suitable conditions for mineral flotation [11]. Hysteresis of the contact angle is commonly observed in these measurements [12]. Such hysteresis means the occurrence of a difference between "advancing" and "retreating" angles. The cause of the hysteresis is the non-ideality of the surfaces with respect to smoothness, rigidity, and homogeneity. In the case of sulfide minerals, another reason for hysteresis can be a reorientation of molecules or groups in the double layer of the solid surface under the influence of the liquid phase. If a bubble is made to advance or retreat, it may meet a different surface from that which it had seen previously. On real surfaces, a hysteresis of 10° or higher is quite common. For example, contact angle hysteresis for water on gold that has sorbed an alkanethiol can be as high as 20° [13]; on silver which has been treated with a solution of di-isobutyl dithiophosphinate in a borate buffer, the hysteresis reaches 45° [14].

The complexity and diversity of the chemical processes accompanying sulfide flotation make it difficult to obtain quantitative relationships. The logical path to the creation of a quantitative theory of sulfide flotation needs the selection of complex physicochemical parameters of the system that (a) react adequately to changes of the flotation conditions and (b) are reproducible. We have studied the wettability of minerals as a function of the electric potential by means of detachment force and induction time measurements. The study was carried out with electrodes made of natural minerals, and the potential was stepped to the required value by means of a potentiostat. This experimental study provided the possibility of determining activation/passivation potentials and, with some approximation, the regions of flotation potentials.

Experimental

Chemicals

Reagent preparation

Potassium xanthates were obtained as commercial products from Hoechst. They were purified according to the standard procedure by two precipitations from acetone by addition of hexane [11]. Fresh stock solutions of xanthate ($5 \cdot 10^{-3}$ M) in borate buffer (pH 9.2, ionic strength 5×10^{-2} M) were prepared daily. Dilutions were made with the borate buffer.

Surface preparation

Discs of natural minerals (Table 1) were manufactured with a diameter of 5–6 mm. These were mounted in fluoroplast holders. The working surface was dry-polished in stages using alumina down to 0.05 μm and rinsed with distilled water or sometimes with ethanol between polishing stages. The surface was repolished immediately before use.

Apparatus and procedure

The set-up used for the measurement of ABDF and ABIT is schematically illustrated in Fig. 1.

Table 1 Properties of mineral samples

Mineral	Formula	Origin	Principal metals content (%)	Mineral impurities	Semiconduction type	Resistivity (Ωm)	Stationary Potential (mV)
Pyrite	FeS_2	Urals	Fe 45.3	Not determined	p	$1.6 \cdot 10^{-2}$	48
Arsenopyrite	FeAsS	Kazakhstan	Fe 34.2, As 44.5	Silica	n	$7 \cdot 10^{-4}$	−15
Chalcopyrite	$CuFeS_2$	Armenia	Cu 22.6, Fe 39.0	Pyrrotite	n	$1.3 \cdot 10^{-3}$	−23
Chalcocite	$Cu_{1.86}S$	Synthetic	Cu 78.8	Not determined	p	$2 \cdot 10^{-4}$	−38
Galena	PbS	Kazakhstan	Pb 86.4	Not determined	n	$1.2 \cdot 10^{-5}$	−60

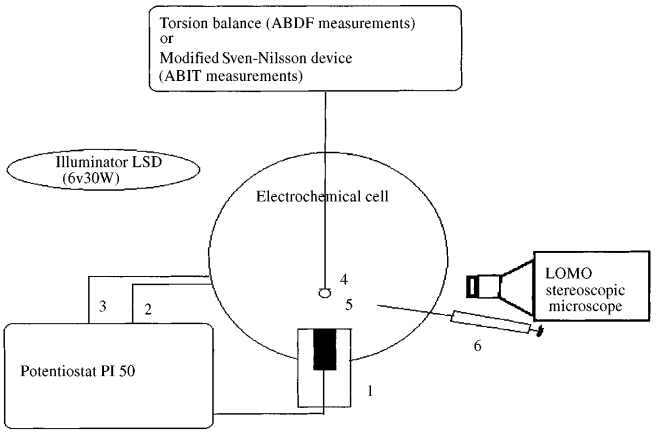

Fig. 1 Principle scheme of the ABIT and ABDF measurements 1 – Mineral electrode; 2 – Reference electrode connection; 3 – Counter electrode connection; 4 – Bubble holder; 5 – Air bubble; 6 – Plug and needle for an air bubble injection.

Electrochemical cells with a three-electrode system were used for all measurements. Potentials were measured and are reported versus a silver-silver chloride reference electrode, which had a potential of +0.22 V against the standard hydrogen electrode. The potential of the mineral electrodes was controlled by a PI 50 (Izmeritel, Gomel, Belaruss) potentiostat programmed with a sweep generator. The working electrode consisted of a mineral disc. A wire connected the disc to the external electrical circuit. The reference electrode was connected to the main compartment through a Lugging probe capillary. Under potentiostatic control, the current passed between the mineral disc and a platinum counter electrode which was housed in the compartment, separated from the main cell by a sintered glass disc.

A torsion balance and a modified Sven-Nilsson device [15] were used for the detachment force and the induction time measurements. Induction time is defined as the minimum time necessary for the attachment of an air bubble to the mineral surface. Air bubbles for measurements were deposited on the holder surface from a small diameter flat-nosed needle positioned below the holder. The bubble formation and size were controlled using a combination of plug and needle. The needle was detached from the bubble before measuring the detachment force or the induction time. The movement of the bubble was observed through the wall of the cell, the latter being illuminated by an electric lamp. The ABDF measurements were made a few seconds after the gas front had ceased to advance across the mineral surface. A freshly polished sample was used for each new reagent. The standard deviations of the ABDF values with five repeated measurements were confirmed to be less than 2 μN.

Results and discussion

Figure 2 shows the effect of butyl xanthate concentration on the ABDF for various sulfides. It shows an increase of the ABDF for xanthate concentrations up to 106 μM. For all minerals except galena, the ABDF values reach their maxima at a concentration of 186–265 μM butyl xanthate. Figure 2 illustrates that wettability of sulfides in the presence of xanthates depends not only on the amount of the collector used but also on the nature of the sulfide mineral. These data do not support the conclusion, based on the contact angle experiments, about equal maxima wettabilities for all surfaces covered by the same xanthate [11].

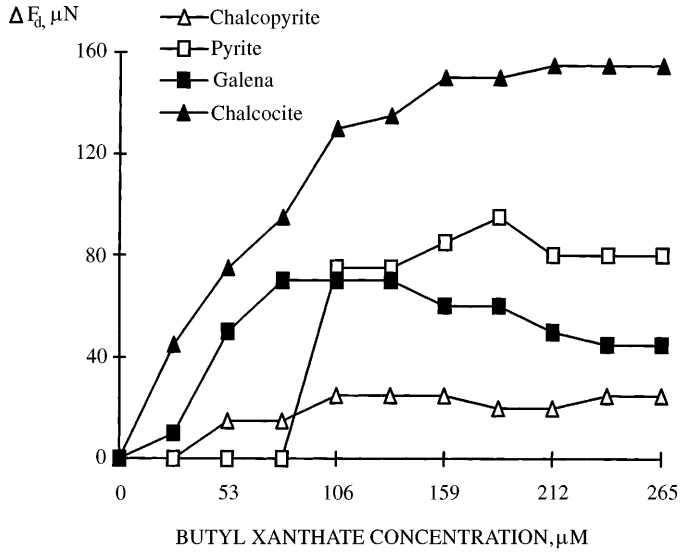

Fig. 2 Influence of xanthate concentration on the detachment force variation in 0.05 M sodium tetraborate solution

In the case of pyrite, the detachment force reaches maximum values at 250–300 μM concentrations of different xanthates. The maximum values exceed the initial values by 80, 100, and 125 μN for butyl, amyl, and hexyl xanthates, respectively. Without polarization, under stationary potential with increasing length of the alkyl chain, we observe an increase of the xanthate concentration at which the detachment force reaches its maximum.

An examination of the effect of xanthate concentration on the induction time exhibits a decrease at a definite concentration (*critical value*). A further rise of the concentration has no effect on the kinetics of adhesion. Adhesion kinetics is influenced by the carbon chain length and by the electrochemical potential of the surface [16]. The growth of the carbon chain from ethyl to amyl resulted in a decrease of the induction time and expanded the range of adhesion potentials (see Table 2). The potentials of ABIT experiments are close to the "bubble input" results obtained for gas advancing (water retreating) conditions [17]. The adhesion potential range obtained by ABIT measurements and by "bubble input" experiments [17] is narrower than that obtained from ABDF and flotation results [18]. In the hexyl-xanthate case the adhesion strength is the largest, but, for the formation of a three-phase contact perimeter, a significant induction time is required. In the presence of long-chain xanthates, the interval of *adhesion potentials* 0.7 V for an induction time less than 5 s. In the experiments with hexyl xanthate, we observed a cathodic shift of adhesion potential of about 200 mV in comparison with the results of the amyl xanthate experiment. Because of the narrow adhesion interval, butyl xanthate as a collector has an advantage for the electrochemical regulation of selective flotation.

Figure 3 summarizes the ABDF potential polarization curves for pyrite. These curves are similar in shape for all the xanthates studied and show two maxima and one

Table 2 The influence of the potential of pyrite electrode and the length of xanthate carbon chain on the air bubble-mineral attachment and the induction time values[a]

Potential (V)	−0.6	−0.5	−0.4	−0.3	−0.2	−0.1	0	0.1	0.2	0.3	0.4	0.5	0.6
Xanthate						ABIT(s)							
Ethyl	No	No	No	No	No	No	>5	5	>5	No	No	No	No
Butyl	No	No	No	No	No	>5	5	3.5	3	3	3	>5	No
Amyl	No	No	No	>5	3.5	3.5	3	0.5	0.5	2.5	4	>5	No
Hexyl	No	>5	5	3.5	3	2	3	2.5	5	>5	No	No	No

[a] Xanthate concentration, 50 mg/dm^3 or 312, 265, 248 and 231 μM for ethyl, butyl, amyl, and hexyl xanthates, respectively
[b] No attachment

minimum. The first maximum, which is the higher one, observed at a potential of about 0.2 V. This corresponds to the potential of the formation of a dixanthogen layer on the surface. The maximum value of the detachment force varies from 290 to 420 μN with increasing length of alkyl chains of the collectors. The next maximum of the detachment force is observed at a potential of about 0.9 V, and its value seems to depend slightly on the xanthate chain length. For all xanthates studied, the detachment forces are within the range 270–310 μN.

On the ABDF potential curves (Fig. 3), a decrease in the ABDF between the maxima was observed. The potentials of the minima are near to 0.5 V. The existence of the minima on the curve of pyrite hydrophobicity characteristics (detachment force, contact angle, flotation recovery) plotted against the potential of the electrochemical polarization qualitatively agrees with the case of the chemical regulation of redox-potential by dithionite addition [18].

If the potential exceeds 0.16 V, a stepwise dissolution of pyrite is observed [19]:

$$FeS_2 + 19\,OH^- \rightleftharpoons Fe(OH)_3 + 2\,SO_4^{2-} + 8\,H_2O + 15\,e \qquad E = 0.2 - 0.075pH \quad (2)$$

$$Fe(OH)_3 + 5\,OH^- \rightleftharpoons FeO_4^{2-} + 4H_2O + 3e \qquad E = 1.41 - 0.1pH \quad (3)$$

After the first reaction, the pyrite surface is covered by hydrophilic iron hydroxide, which leads to an increase of the resulting wettability. The ranges of adhesion potentials obtained by ABDF measurements correlate with the data of floatability-potential for pyrite [18].

Figures 4 and 5 depict the results obtained in measurements of the ABDF at the surfaces of galena and chalcocite for xanthates with different lengths of the hydrocarbon chain and at various potentials of electrochemical polarization. For galena, stable adhesion is observed in the potential range of thermodynamic stability of lead sulfide, with a maximum force of detachment at potentials 100–150 mV greater than the stationary value (Table 1). A further increase of the anodic polarization potential leads to a sharp decrease of the ABDF

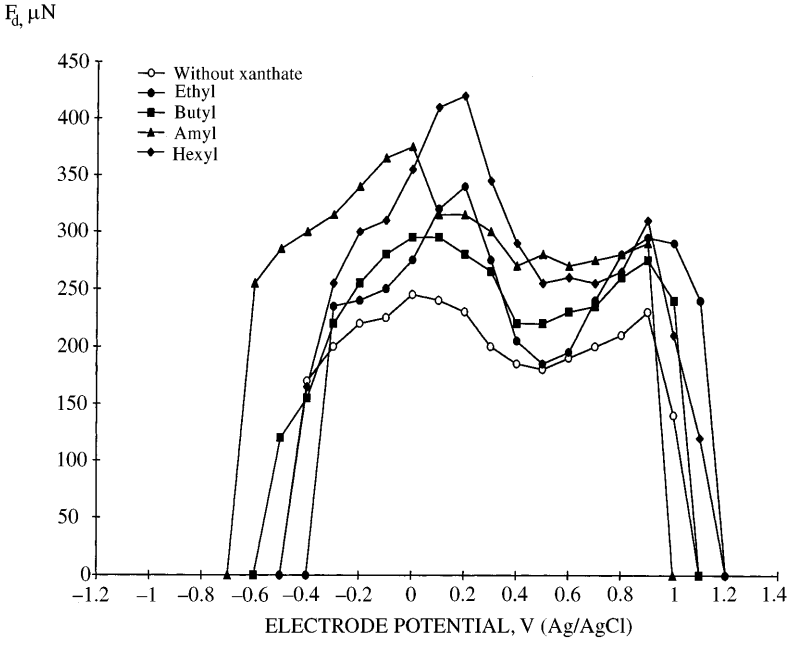

Fig. 3 Dependence of the ABDF on the potential of pyrite electrode in 0.05 M sodium tetraborate solution containing 50 mg/dm^3 or 312, 265, 248 and 231 μM of ethyl, butyl, amyl, and hexyl potassium xanthates, respectively. Reference electrode Ag/AgCl/KCl (sat)

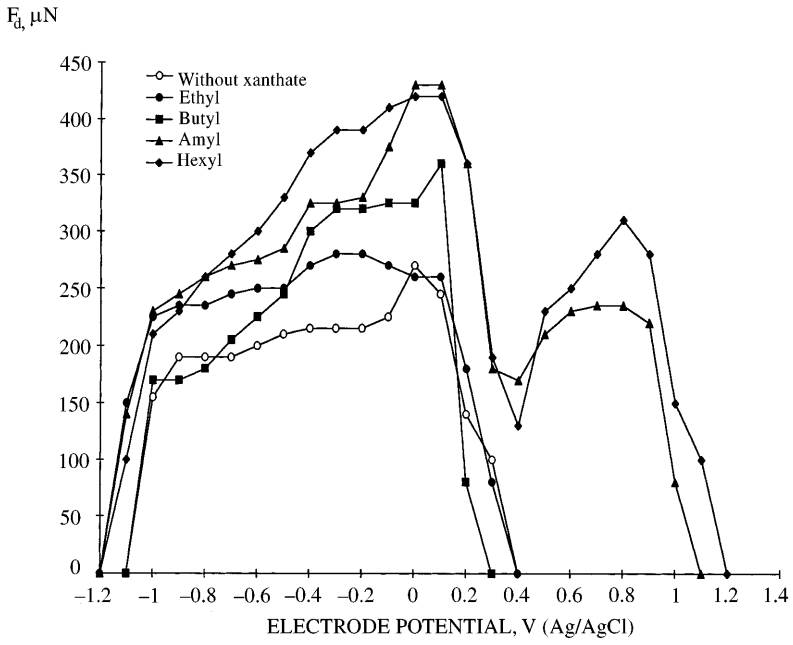

Fig. 4 Dependence of the ABDF on the potential of galena electrode in 0.05 M sodium tetraborate solution containing 50 mg/dm^3 or 312, 265, 248 and 231 μM of ethyl, butyl, amyl, and hexyl potassium xanthates, respectively. Reference electrode Ag/AgCl/KCl (sat)

and a detachment of the bubble. The rapid decrease of floatability at potentials above 0.15 V was explained by Trahar on the basis of a possible decomposition of lead xanthate as a result of the following reaction [18]:

$$PbX_2 + 2\ H_2O = HPbO_2^- + X_2 + 3H^+ + 2\,e. \qquad (4)$$

When the larger xanthates (amyl and hexyl) are applied to galena, a second region of stable adherence appears at potentials of 0.4–1.2 V. In this region of potentials, air bubble attachment is also observed when a lead electrode is used, not only with the amyl and hexyl xanthates but also with butyl xanthate.

For chalcocite, as illustrated in Fig. 5, the greatest increase of the ABDF is observed in the region of the thermodynamic oxidation of copper sulfide. The potentials of these maxima correspond to the oxidation of xanthate ions to dixanthogen. A similar, very distinct maximum of hydrophobicity at potentials of 0.1–0.3 V is also observed for copper. In the flotation of copper sulfides, the sorption of both the metal xanthate and the dixanthogen are important. The additional formation of dixanthogen on the copper sulfide surface increases the force of detachment by 100–150 μN. In the potential range of 0.4–1.0 V, only dixanthogen remains on the surface of the chalcocite electrode, and the ABDF drops to a level characteristic for the coverage of the surface with metal xanthate only. The ranges of adhesion potentials obtained by ABDF measurements for galena (−1 to 0.2 V) and chalcocite (−0.5 to 1.2 V) (cf. Figs. 4 and 5) correlate with the potential ranges of floatability for galena (<0.2 V) and chalcocite (>-0.4 V), which are suitable for the chemical regulation of the redox potential by sodium dithionite addition [18].

For the sulfides studied, we observe an increase of the ABDF with increasing length of the hydrocarbon chain. In the potential ranges for stable adhesion, the average values of the ABDF increase exponentially (galena and chalcopyrite) or linearly (pyrite) with increasing length of the hydrocarbon chain of the xanthate. For galena and chalcopyrite, the ABDF increases according to the equations:

$$y = \exp(0.3075x) \times 8.312 \qquad (5)$$

and

$$y = \exp(0.4434x) \times 2.867 \qquad (6)$$

respectively, where x is the number of carbon atoms in the alkyl chain.

With increase in alkyl chain length, the cathodic limit of the adhesion potential shifts to higher values (see Fig. 5). The direction of this shift agrees with the order of the standard oxidation potentials of xanthate to dixanthogen for different xanthates. A cathodic shift of 90 mV was reported for the start of the pyrite flotation when the ethyl xanthate was replaced by butyl xanthate [17].

Figure 6 illustrates the cathodic boundaries of adhesion potentials in butyl (a) and amyl (b) xanthate solutions for various minerals. The potential variation corresponds to the sequence of stationary potentials of sulfide minerals [20], the stationary potentials data of Table 1 (except arsenopyrite), and the order of the flotation potentials [21]. One of the reasons for the observed differences in the potential values of the ABDF experiments of Fig. 6 and those of [21] is the direction of scanning of the potential. In [21], the electrochemical potential was scanned from reduction to oxidation potentials. In Fig. 6 ABDF experiments the potential was changed from stationary values to reduction potentials. Richardson and Walker observed hysteresis in the flotation response obtained in the two different directions

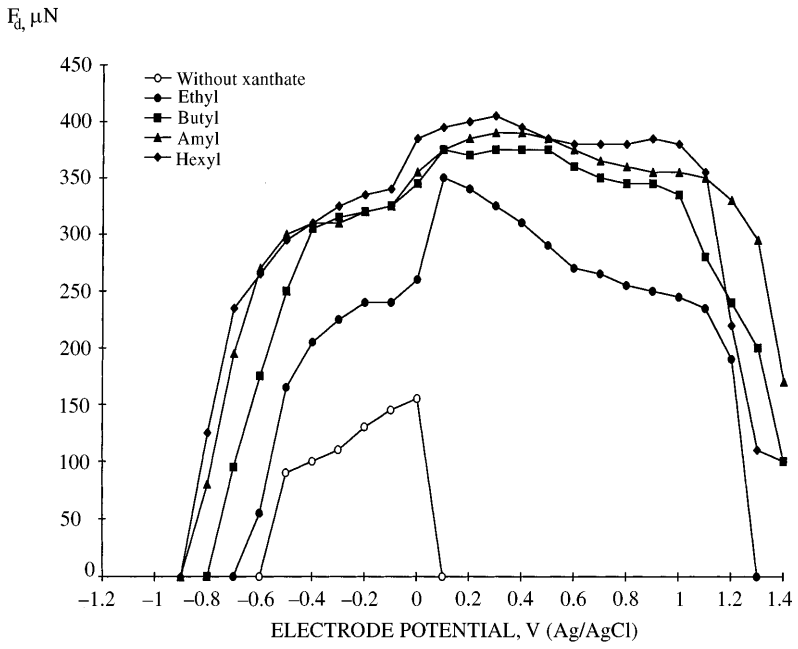

Fig. 5 Dependence of the ABDF on the potential of chalcocite electrode in 0.05 M sodium tetraborate solution containing 50 mg/dm^3 or 312, 265, 248 and 231 μM of ethyl, butyl, amyl, and hexyl potassium xanthates, respectively. Reference electrode Ag/AgCl/KCl (sat)

of potential scanning [21]. The hysteresis was such that during reduction the flotation edge shifted to more negative values.

Numerous studies of redox reactions occurring on the surfaces of sulfide minerals in alkaline solutions show that under anodic polarization of sulfides, starting from the stationary potential, oxidation has occurred, yielding metal oxides and different forms of sulfoxide compounds [1, 2, 6–8, 17–21]. In electrochemical experiments, sulfur is oxidized to sulfate with large overpotentials [1]. Cathodic polarization leads to electroreduction of dissolved oxygen and sulfide decomposition, with production of sulfide ion and metal. At currentless potentials, the surface of sulfide minerals is covered by sulfur, metal-deficient metal sulfides, or metal hydroxides. Sulfide minerals must be rendered highly hydrophobic before significant flotation can occur. The following simplified scheme summarizes the redox changes of sulfide surfaces in the presence of xanthate in correspondence with ABDF curves:

Composition of the surface of sulfide electrodes

$$\text{Me} \leftarrow \text{MeS} \rightarrow \text{MeS; S; MeX} \rightarrow \text{MeS; MeX; X}_2 \rightarrow \text{MeSO}_4; \text{X}_2 \rightarrow \text{Me(OH)}; \text{X}_2 \rightarrow \text{Me(OH)}$$

Air bubble detachment force

$$\text{Min I} \leftarrow \text{Max I} \rightarrow \text{Max II} \rightarrow \text{Min II} \rightarrow \text{Max III} \rightarrow \text{Min III}$$

An electrochemical study of the influence of the potential of the mineral electrode on the detachment force confirms the flotation results [8, 10]. It was found, for example, that the cathodic pre-treatment of pulp at −0.6 to −0.8 V depressed pyrite, thus making it possible to improve selective flotation operations in which pyrite remains in the chamber product. Cathodic pre-treatment of Pb-Cu concentrate at −0.4 to −0.6 V depresses copper minerals and leads to increase in the flotation rate and metal recovery. Anodic pre-treatment of pulp at 0.4–0.6 V improves floatability of copper sulfides.

We can expect only a qualitative correspondence between the potentials in bulk and powder mineral polarization experiments. Furthermore, it is difficult to compare quantitatively the results for various samples of sulfide minerals because of the essential differences in both the electrochemical behaviour and the floatability [22]. A possible way to distinguish differences between real flotation involving particle-bubble attachment and mechanical carryover could be the use of the mono-bubble Hallimond tube technique [23].

Conclusions

1. The experimental methods for the determination of surface wettability can be subdivided into two groups with respect to the direction of the relative motion of liquid and gas phases:
A. Advancing angle for liquid, retreating angle for gas, ABDF
B. Retreating angle for liquid, advancing angle for gas, ABIT.
Quantitative comparisons of the experimental values are possible only within each group.
2. The potentials of electrochemical hydrophilization of the sulfide electrodes increase with increasing length of the hydrocarbon chain of the xanthate: ethyl < butyl < amyl < hexyl.

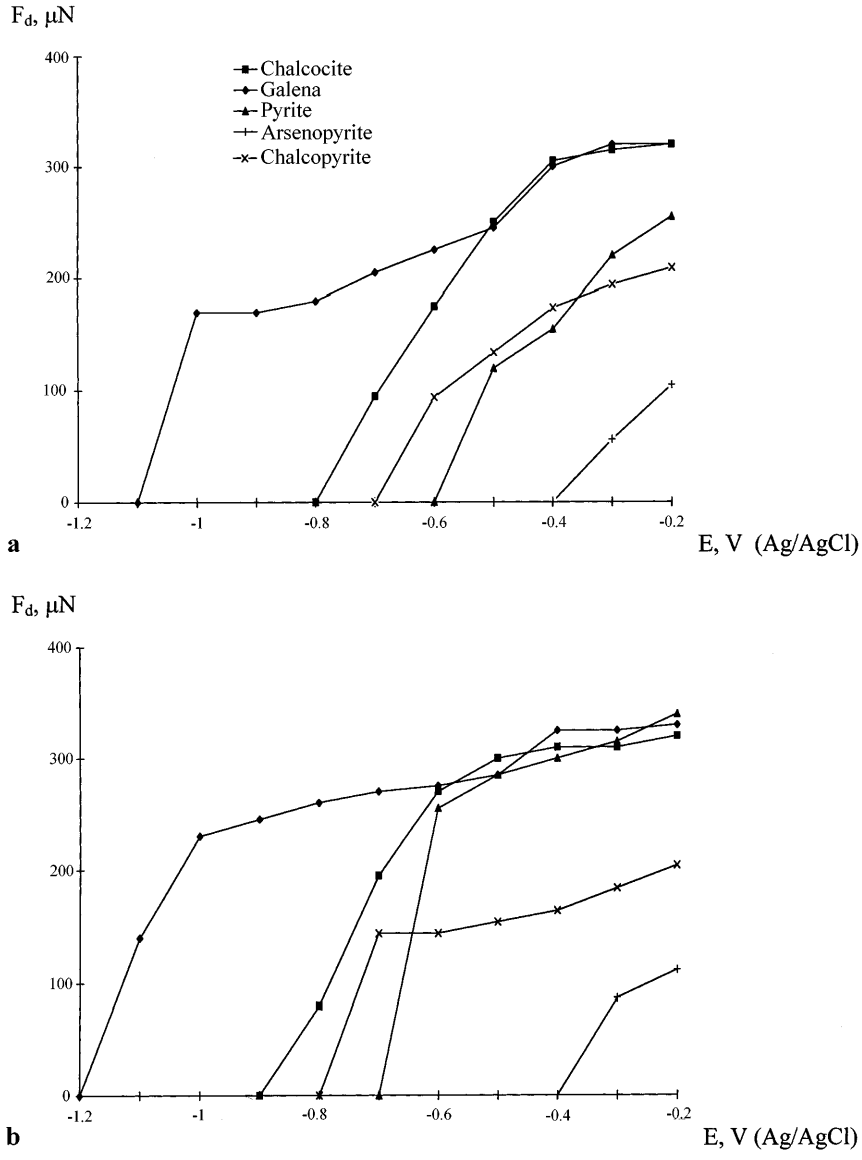

Fig. 6a,b Cathodic parts of ABDF-potential curves for butyl (**a**) and amyl (**b**) xanthates

In the region of potentials for stable adhesion, the ABDF increases exponentially (galena and chalcopyrite) or linearly (pyrite) with increasing length of the hydrocarbon chain of the xanthate.

3. Without any xanthate, an increase of the electrochemical potential by 50–70 mV from the stationary value leads to a maximum decrease of wettability and an increase of natural floatability.

4. In the presence of xanthates, the potentials of cathodic electrochemical hydrophilization of the studied sulfides decrease in the sequence: galena > chalcocite > chalcopyrite > pyrite > arsenopyrite.

5. In the conditions of flotation, the probability of formation of air bubble-mineral particle aggregates by direct collisions is low in view of comparably large values of ABIT. The mechanism of micro-bubble evolution on solids from the supersaturated solution seems to be preferable.

6. Froth flotation results correlate better with conditions for the destruction of bubble-particle aggregates. For the froth flotation modeling, measurements of water phase advancing and gas phase retreating (advancing angles for drops, retreating angles for bubbles, ABDF, etc.) are preferable.

Acknowledgements This work was partially supported by the Russian Foundation of Fundamental Sciences (No. 95-05-4180). The authors wish to thank Prof. Fritz Scholz for useful discussions.

References

1. Peters E (1977) In: Bockris J O'M, Rand DAJ, Welch BJ (eds) Trends in electrochemistry. Plenum, New York, pp 267–290
2. Woods R (1981) In: Bockris J O'M, Conway BE, Yeager E, White RE (eds) Comprehensive treatise of electrochemistry, vol 2. Plenum, New York, pp 571–595

3. Pillai KC, Bockris J O'M (1984) J Electrochem Soc 131: 568
4. Young T (1805) Trans R Soc London 95: 65
5. Kabanov B, Frumkin A (1933) Z Phys Chem A166: 316
6. Radiushkina KA, Vigdergauz VE, Tarasevich MR, Chanturiya VA (1986) Sov Elchem 22: 1491
7. Scholz F, Lange B (1992) Trends Anal Chem 11: 359
8. Vigdergauz VE, Chanturiya VA, Faidel VV, Gromova NK, Yagodkina NG (1992) In: Modern process mineralogy and mineral processing. Beijing, pp 513–519
9. Vigdergauz VE (1989) In: Dobby GS, Rao SR (eds) Processing of complex ores. Pergamon, New York, pp 147–156
10. Vigdergauz VE, Chanturiya VA, Faidel VV (1987) Nonferrous metals 62: 79
11. Sutherland KL, Wark IW (1955) Principles of Flotation. AIMM, Melbourne
12. Freundlich H (1923) Colloid and capillary chemistry. Dutton, New York
13. Folkers JP, Laibinis PE, Whitesides GM (1992) J Adhes Sci Technol 6: 1397
14. Farinato RS, Nagaraj DR (1992) J Adhes Sci Technol 6: 1331
15. Sven-Nilsson I (1935) Ing Vetenskaps Akad Handl 133
16. Vigdergauz VE, Chanturiya VA, Nedosekina TV (1996) Fizykochem Probl Miner 30: 187
17. Gardner JR, Woods R (1977) Aust J Chem 30: 981
18. Trahar WJ (1984) In: Jones MH, Woodcock JT (eds) Principles of mineral flotation. Parkville, pp 117–135
19. Radiushkina KA, Vigdergauz VE, Tarasevich MR, Chanturiya VA (1986) Sov Elchem 22: 1394
20. Allison SA, Goold LA, Nicol MJ, Granville Al (1972) Metallurg Trans 3: 2613
21. Richardson PE, Walker GW (1985) The flotation of chalcocite, bornite, chalcopyrite, and pyrite in an electrochemical-flotation cell. In: XVth Int Mineral Processing Congress, Cannes, vol 2, pp 198–210
22. Chmielewski T, Nowak P (1992) Fizykochem Probl Miner 25: 59
23. Drzymala J (1994) Int J Miner Process 42: 153